Sustainable Environment Research

RESEARCH Open Access

Removal of aqueous carbamazepine using graphene oxide nanoplatelets: process modelling and optimization

Sandipan Bhattacharya[1], Priya Banerjee[2], Papita Das[1,3*], Avijit Bhowal[1,3], Subrata Kumar Majumder[4] and Pallab Ghosh[4]

Abstract

Unplanned and unmonitored developmental activities have resulted in a rapid emergence of pollutants like pharmaceuticals and personal care products (PPCPs) in the environment. These PPCPs are considered as potential health hazards. A wide variety of physical, biological and chemical processes are presently being investigated for ensuring the efficient removal of such pollutants from effluents. The present study investigates the potential of graphene oxide nanoplatelets (GONPs) for removal of a common and extensively used drug, Carbamazepine (CBZ) from aqueous solutions. Batch studies were performed to assess the potential of graphene oxide for adsorption of CBZ under different conditions of initial CBZ concentration, adsorbent dosage, temperature and solution pH. Process optimization was performed using Response Surface Methodology and Artificial Neural Network modelling. Results obtained indicated 99% CBZ removal under optimum solution pH, adsorbent dosage and treatment duration of 6, 1 g L^{-1} and 120 min respectively. Results revealed that CBZ adsorption by GONPs followed Temkin isotherm and pseudo second order kinetics. A subsequent reusability study established that the GONPs could be reused for up to 8 times without any loss of adsorption efficiency. Therefore, it can be concluded that graphene oxide reported herein has immense potential for adsorption of trace organic pollutants from aqueous phases.

Keywords: Emerging pollutants, Graphene oxide, Carbamazepine, Adsorption, Wastewater treatment

Introduction

Pharmaceutical wastes present in effluents are rapidly becoming issues of immense concern on a global scale [1]. Wide use and disposal of these products have resulted in a rapid rate of accumulation of the same in adjacent aquatic environments [2, 3]. Carbamazepine (CBZ; $C_{15}H_{12}N_2O$) is one such widely consumed antiepileptic drug which is primarily prescribed as sedative to patients suffering from depression, post-traumatic stress disorder, restless leg syndrome, diabetes insipidus, pain and neurological syndromes [4–6].

Previous studies have reported a global yearly CBZ usage of approximately 1.01 kt. Such substantial usage of CBZ has resulted in its appearance in different sources of water including surface water, ground water, wastewater treatment plants and even drinking water. Therefore, presence of CBZ in different water resources is being considered as an issue of global concern [7–14]. CBZ reportedly exerts toxic effects on aquatic life including bacteria, algae, invertebrates and fish [15]. Permissible limit of CBZ in drinking water sources varies in different countries and is found to be 40 and 100 μg L^{-1} in Minnesota, U.S and Australia respectively [16]. Moreover, use of water bearing CBZ for irrigation results in accumulation of the same in soil [17]. The standard concentration of CBZ in soils irrigated using wastewaters has been found to be 0.02–15 μg kg^{-1} [18]. According to the US Food and Drug Administration, an environment

* Correspondence: papitasaha@gmail.com
[1]Department of Chemical Engineering, Jadavpur University, Kolkata 700032, India
[3]School of Advanced Studies in Industrial Pollution Control Engineering, Jadavpur University, Kolkata 700032, India
Full list of author information is available at the end of the article

assessment should be performed whenever the concentration of the active ingredient of CBZ is equal to or found to exceed 1.0 μg L^{-1} in aquatic environment [16]. Hence, efficient treatment strategies are required for removal of this pollutant from the aquatic environment.

However, conventional treatment processes practised in wastewater treatment plants (WWTPs) are capable of removing only 32–35% of trace pollutants like CBZ from wastewaters [8, 19]. High persistence of CBZ may have resulted in discharge of the same from WWTPs without undergoing biodegradation or transformation [19]. According to Zhang et al. [7], CBZ concentration of approximately 10 ng L^{-1} has been found in drinking water samples collected from Berlin. Effluents bearing pharmaceutical wastes have been reportedly treated with conventional processes like oxidation, ozonation, photocatalysis of exposure to UV, etc. [20]. However, these processes have yielded only partial degradation of pharmaceuticals or resulted in the formation of carcinogenic or toxic end products like dioxins, chlorinated phenols, trihalomethanes, chlorinated phenoxyphenols, etc. [20].

Recent studies have reported the process of adsorption as an efficient and cost-effective process for persistent contaminant treatment [21–23]. A wide variety of materials such as clays, polymers and several carbon-based materials (like fly-ash or charcoal) have been investigated for adsorption of different types of aqueous pollutants [23]. Of all other types of carbonaceous adsorbents reported in contemporary studies, graphene oxide (GO) has received significant attention due to its mechanical and chemical stabilities as well as high specific surface area [23]. Carbonaceous nanomaterial like GO has been widely investigated as an adsorbent due to its convenient process of synthesis, efficient pollutant removal in significantly low dosage and cost effectiveness [24–26]. Moreover, GO surfaces bear large quantities of oxygen rich epoxy, hydroxyl, and carboxyl groups [23]. Presence of these functional groups render GO hydrophilic and therefore, suitable for adsorption of pharmaceuticals from their aqueous solutions [23].

The present study investigated the potential of GO nanoplatelets (GONPs) for efficient removal of CBZ. Morphology, chemical nature and crystalline properties of GONPs used in this study were analysed with scanning electron microscopy (SEM), Fourier transform infrared (FTIR) spectroscopy, X-ray diffractometry (XRD), respectively. Batch studies were carried out for elucidating the effect of significant experimental parameters on the process of adsorption. Results obtained in batch studies were further investigated for determining the isotherm and kinetic models guiding the concerned process. Process optimization was carried out using response surface methodology (RSM) and artificial neural network (ANN) on a comparative scale. Consecutive adsorption-desorption cycles were also performed for determining the reusability potential of the GONPs reported in this study.

Experimental methodology

Materials

All chemicals (analytical grade) used in this study were purchased from Merck, India and used without additional purification. CBZ (λ_{max} = 283 nm) and potassium bromide (KBr; FTIR grade) used in this study were purchased from M.P. Biomedicals, India. Residual CBZ concentrations were determined using a UV-Vis spectrophotometer (Lambda 365; Perkin Elmer).

GONP synthesis

GONPs were synthesised using modified Hummer's method as described by Banerjee et al. [26]. The GONPs so prepared were consecutively washed using HCl (5%), ethanol (30%) and distilled water. Finally, GONPs having neutral pH were obtained by centrifugation, dried in a vacuum oven, ground, sieved and stored for future use [27].

Characterization of GONPs

GONP morphology was examined with a SEM (Zeiss EVO-MA 10, Germany). Samples for SEM analysis were rendered conductive by coating the same with platinum using a sputter coater. GONP samples were also analysed using a FTIR Spectrometer (Perkin Elmer, USA) for identifying the functional groups present on the adsorbent surface. For FTIR spectroscopic analysis, samples were cast into pellets using KBr whereby the ratio of KBr:GONP was 100:1 (w/w). FTIR spectrums were recorded in terms of % transmittance within a range of 400–4000 cm^{-1} with a resolution of 4 cm^{-1}. The crystalline properties of GONP samples were analysed using an XRD (Malvern Panalytical, UK). XRD analysis was performed with 30 mA current, 40 kV voltage and a CuK radiation of 1.5406 nm within the range of 5–80° (2θ) [28].

Batch studies

Batch studies for investigating the effect of experimental parameters on CBZ adsorption potential of GONPs were carried out in 250 mL Erlenmeyer flasks with a continuous agitation of 100 rpm. Experimental parameters considered for this study included initial CBZ concentration (1–20 mg L^{-1}), adsorbent dosage (0.25–1 g L^{-1}), pH of adsorbate solution (2–10) and temperature (25–40 °C). Each study was carried out for 90 min.

Optimization of the process by RSM

The concerned process was optimized with the central composite design (CCD) parameter of RSM using the software Design Expert Version 7.0 (Stat-Ease, USA). RSM is an integrated mathematical and statistical tool for process optimization and elucidation of effects of inter-parameter interactions on the concerned process [29]. Process optimization is performed n the basis of a number of experiments (called runs) recommended by RSM. For these runs, specified ranges of selected experimental parameters are provided as input variables. Results obtained for these experiments are considered as output response [29]. RSM decreases cost by reducing repetitive and expensive methods of analysis and resultant numerical noise. In this study, process optimization was carried out in terms of experimental parameters like pH of the adsorbate solution, adsorbent dosage ($g\,L^{-1}$) and duration of treatment (min). All experiments were performed with solutions having a CBZ concentration of $5\,mg\,L^{-1}$. Output of this study was recorded in terms of % CBZ removal by GONPs. Details of these factors are shown in Table 1. On the basis of this 3-factor model, the software recommended 20 experiments (including 6 replications) as enlisted in Table 1.

ANN modelling

The ANN program is an analogous distributed information structure for processing consisting interconnected units of processing [29]. The ANN program has been developed on the basis of knowledge available regarding the biological nervous systems [29]. ANN is widely investigated as a mathematical and computational tool for process optimization. ANN reportedly scores over traditional processes of optimization as it is devoid of complex processes incurred by the latter [22]. In this study, CBZ adsorption by GONP was modelled with a triple layer ANN model interconnected by virtue of linear transfer

Table 1 Experimental details and results obtained for RSM (CCD) based optimization of Carbamazepine (CBZ) adsorption by graphene oxide (GO)

Factors	Units	Levels			Star point α = 1.68	
		Low (−1)	Central (0)	High (+ 1)	-α	+α
A: pH		4	6	8	5.32	8.68
B: Adsorbent dosage	$g\,L^{-1}$	0.26	0.63	1.00	0.005	1.255
C: Time	min	60	90	120	40	141
Run	Factors			Predicted % CBZ removal	Experimentally recorded % CBZ removal	
	A	B	C			
1	8	1.00	120	52	52	
2	2	1.00	120	99	99	
3	6	0.63	90	78	78	
4	6	0.26	120	52	51	
5	4	0.63	90	74	73	
6	6	0.63	90	78	77	
7	4	1.00	60	70	70	
8	8	0.26	120	47	47	
9	6	0.63	140	60	61	
10	6	0.63	90	78	78	
11	6	0.63	39	49	48	
12	8	0.26	60	63	62	
13	8	1.00	60	68	69	
14	6	0.01	90	34	35	
15	6	0.63	90	78	78	
16	4	0.26	60	23	24	
17	6	1.25	90	78	77	
18	6	0.63	90	78	78	
19	9	0.63	90	68	69	
20	6	0.63	90	78	78	

functions that was developed on the basis of a back-propagation schema. The ANN model used in this study was created using MATLAB 7 [30, 31]. Different transfer functions like 'poslin', 'purelin' and 'traincgp' were analysed in this study for guiding the developed model. The schematic flow diagram of the multilayer feed forward ANN model developed in this study is shown in Fig. 1. The input layer consisted of the independent variables like pH solution, adsorbent dosage ($g\,L^{-1}$), and duration of treatment (min). Output layer of this model consisted of the dependent variable like percentage removal of CBZ from its aqueous solutions. The most ANN model was developed by a trial and error approach on the basis of the 14 unique experimental combinations recommended by RSM.

Reusability study

The reusability potential of GONPs used in this study was assessed by means of subsequent adsorption - desorption studies. Post adsorption studies, GO was retrieved and treated separately using four mediums namely deionised water, NaOH (10% (v/v) aqueous solution), HCl (10% (v/v) aqueous solution), and NaCl (0.10 $mg\,L^{-1}$). After treatment, the level of CBZ in the desorbing solutions was measured using a spectrophotometer. The regenerated GO was used for another round of CBZ adsorption. The adsorption - desorption study was repeated for up to 10 cycles.

Calculations

Percentage removal of CBZ and equilibrium CBZ concentration

Throughout the batch study, samples were collected after predetermined intervals of 15, 30, 45, 60 and 90 min, centrifuged and the resultant supernatants were analysed for residual CBZ concentrations using the following formula.

$$Removal\ \% = \frac{(C_0 - C_t) \times\ 100}{C_0} \tag{1}$$

where C_o and C_t represent initial CBZ concentration ($mg\,L^{-1}$) and CBZ concentration in the experimental solution after time t ($mg\,L^{-1}$), respectively.

Maximum adsorption capacity, q_e, ($mg\,g^{-1}$) after a pre-determined time interval was determined using the following formula.

$$qe = \frac{((C_{i\,-}\,C_v\ ) \times V)}{m} \tag{2}$$

Analysis of process isotherms

Results obtained from batch studies conducted over variable adsorbent dosage (0.25, 0.50, 0.75 and 1.00 $g\,L^{-1}$) were subjected to analysis of different isotherm models [32–34]. The equations, plots, values of different isotherm parameters and respective correlation coefficients (R^2) are presented in the Table 2.

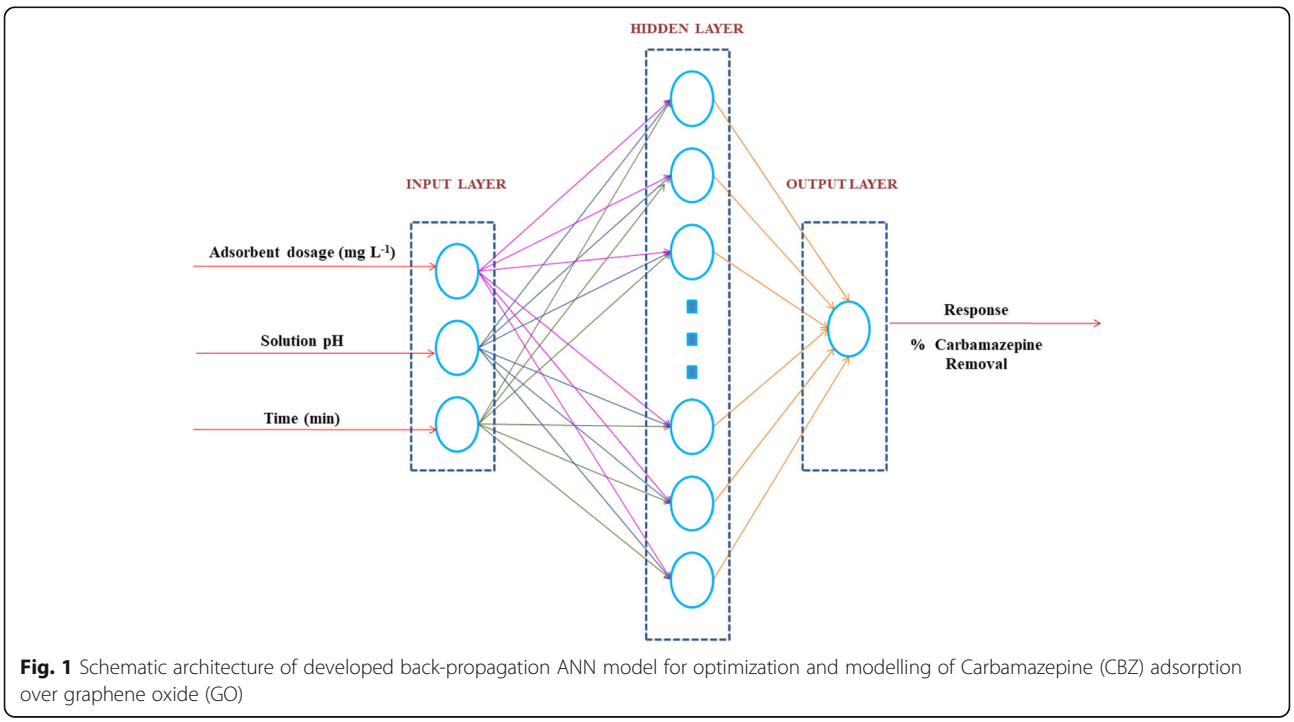

Fig. 1 Schematic architecture of developed back-propagation ANN model for optimization and modelling of Carbamazepine (CBZ) adsorption over graphene oxide (GO)

Table 2 Isotherm parameters for Carbamazepine (CBZ) adsorption by graphene oxide nanoplatelet (GONP)

Models	Description	Unit	Result obtained at an adsorbent dosage of 1 g L^{-1}
Langmuir $\frac{C_e}{q_e} = \frac{1}{Q^0 b} + \frac{C_e}{Q^0}$	Equilibrium CBZ concentration in solution	mg L^{-1}	0.065
	Theoretical maximum adsorption capacity	mg g^{-1}	2.47
	Maximum monolayer coverage capacity calculated from slope of C_e/q_e vs. C_e plot.	mg g^{-1}	0.80
	Langmuir coefficient of energy of adsorption calculated from intercept of C_e/q_e vs. C_e plot.	L mg^{-1}	0.50
	Correlation coefficient		0.914
Freundlich $\ln q_e = \frac{1}{n_f} \ln C_e + \ln K_f$	Adsorption intensity calculated from slope of ln q_e vs. ln C_e plot		4.02
	Freundlich coefficient of adsorption capacity calculated from intercept of ln q_e vs. ln C_e plot	mg g^{-1}	1.49
	Correlation coefficient		0.709
Temkin $q_e = B_T \ln C_e + B_T \ln K_T$	Coefficients of heat of adsorption calculated from slope of q_e vs. ln C_e plot at operational temperature T (308 K)	J mol^{-1}	0.39
	Temkin equilibrium binding constant calculated from intercept of q_e vs. ln C_e plot at operational temperature T (308 K)	L g^{-1}	64
	Correlation coefficient		0.815
Dubinin-Radushkevich $\ln q_e = \ln Q_s - B\varepsilon^2$	Dubinin–Radushkevich constant calculated from slope of ln q_e vs. ε^2 plot.	mol^2 kJ^{-2}	1.0E-08
	Theoretical isotherm saturation capacity calculated from intercept of ln q_e vs. ε^2 plot.	mg g^{-1}	0.30
	Polanyi potential		7071
	Correlation coefficient		0.402

In the equation of the Dubinin-Radushkevich isotherm, ε known as the Polanyi potential, was calculated from the equation given as follows [23].

$$\varepsilon = RT \ln\left(1 + \frac{1}{C_e}\right) \tag{3}$$

whereby, C_e represents residual CBZ concentration under equilibrium conditions.

Analysis of process kinetics

Results obtained from batch studies conducted over a range of temperatures (25, 30, 35 and 40 °C) were subjected to analysis of different kinetic models [35–38]. The equations, plots, values of different kinetic parameters and R^2 are presented in the Table 3.

The activation energy, E_a, (J mol^{-1}) for CBZ adsorption by GONP was determined using the Arrhenius equation given below [39].

$$\ln k = \ln A - \frac{E_a}{RT} \tag{4}$$

whereby, k, A, R and T indicate the kinetic constant, the pre-exponential factor, the ideal gas constant (8.314 J mol^{-1} K^{-1}) and experimental temperature (K) respectively. The activation energy of the concerned process was calculated from the slope of the Arrhenius plot (ln k vs. T^{-1} plot).

Analysis of process thermodynamics

Process thermodynamics guiding CBZ adsorption by GONP was analysed in terms of changes in Gibbs free energy (ΔG°; kJ mol^{-1}), enthalpy (ΔH°; kJ mol^{-1}) and entropy (ΔS°; J mol^{-1} K^{-1}). These parameters were evaluated using the equations given as follows [23]:

$$K_c = \frac{C_a}{C_e} \tag{5}$$

$$\Delta G^\circ = -RT \ln K_c \tag{6}$$

$$\Delta G^\circ = \Delta H^\circ - T\Delta S^\circ \tag{7}$$

where, K_c and C_a denote distribution coefficient of adsorption and amount of CBZ adsorbed/unit mass of GONP (mg g^{-1}), respectively. The slope and intercept of the ΔG° vs T plot were used for calculating ΔH° and ΔS° respectively.

Table 3 Kinetic parameters for Carbamazepine (CBZ) adsorption by graphene oxide nanoplatelet (GONP)

Models	Description	Units	Result obtained at a temperature of 40 °C
Pseudo 1st order $\log(q_e - q_t) = [\log q_e - \frac{k_1}{2.303}$ t]	Pseudo-1st order rate constant obtained from linear plots of *log* $(q_e - q_t)$ vs. *t*.	min^{-1}	0.0018
	Quantity of CBZ adsorbed at equilibrium	mg g^{-1}	8.8
	Correlation coefficient		0.685
Pseudo 2nd order $\frac{t}{q_t} = \frac{1}{k_2 q_e^2} + \frac{t}{q_e}$	Pseudo-2nd order rate constant determined from plot of t/q_t vs. *t*.	mg g^{-1} min^{-1}	0.0023
	Quantity of CBZ adsorbed at equilibrium	mg g^{-1}	5.77
	Correlation coefficient		0.998
Intraparticle diffusion $q_t = K_{diff} t^{1/2} + C$	Intra-particle diffusion rate constant calculated from the slope of regression plot of q_t vs. $t^{1/2}$ where *t* is time (min).	mg g^{-1} $min^{-1/2}$	0.32
	Constant calculated from the intercept of regression plot of $q_t$vs. $t^{1/2}$ where *t* is time (min).	mg g^{-1}	0.11
	Correlation coefficient		0.914
Elovich $q_t = \frac{1}{\beta} \ln(\alpha\beta) + \frac{1}{\beta} \ln(t)$	Initial adsorption rate constant calculated from the intercept of liner plot of q_t vs. *ln t*	mg g^{-1} min	5.78
	Initial desorption rate constant calculated from the slope^{-1} of liner plot of q_t vs. *ln t*.	mg g^{-1}	0.98
	Correlation coefficient		0.965

Optimization using RSM

The appropriate model facilitating maximum efficiency of the concerned process was identified by analysis of variance and was found to be quadratic polynomial in nature. The empirical association of the three independent variables selected for this study was determined from the quadratic polynomial equation given as follows.

$$Y = m_0 + \sum_{i=1}^{k=3} m_i x_i + \sum_{i=1}^{k=3} \sum_{j=1}^{k=3} m_{ij} x_i x_j + \sum_{i=1}^{k=3} m_{ii} x_i^2 + e \quad (8)$$

whereby, Y represents response (dependent variable), m_0 indicates constant coefficient, m_α (α = i,j,ij) denotes regression coefficients of linear, quadratic and interaction models, respectively, x_α (α = i,j) indicates experimental parameters (independent variables) and e denotes error.

Statistical calculations

All experiments were repeated thrice and results expressed as Mean ± SD. All results were analysed using Microsoft Excel 2007. Statistical significance of data used in RSM and ANN analysis were determined with Design Expert, Version 7 (Minneapolis, USA) and MATLAB 7 (USA) respectively.

Results and discussion

Characterization of the adsorbent

Figure 2a exhibits the surface morphology of GONP as recorded using SEM. The SEM images of GONP revealed that it is composed of thin, closely associated and highly overlapping platelet-like carbon sheets. The rough surfaces of these crumpled GONPs reportedly facilitate efficient adsorption [40–42]. These wrinkled and layered structures of GO are reportedly formed as a result of interactions between oxygen containing functional groups [37].

According to the FTIR spectrum of GONP shown in Fig. 2b, peaks recorded at 3365, 1728, 1613, 1386 and 1059 cm^{-1} indicated C=O, C=C, C-H and C–O stretching vibrations respectively. These peaks are reportedly considered as the characteristic peaks of GO [43–45].

The XRD spectra shown in Fig. 2c exhibit three prominent peaks at 12.7°, 25.6° and 42.6° (2θ). These peaks are considered as the characteristic peaks of GONPs [21, 23, 27, 41].

Batch studies

Effect of initial CBZ concentration on adsorption efficiency

Adsorption efficiency of GONPs was found to increase with corresponding increase in CBZ concentration from 1 to 5 mg L^{-1} (Fig. 3a). According to previous reports, this has occurred due to the availability of the active adsorption sites on the surface of GONP [22, 46]. However, a further increase in CBZ concentration beyond 5 mg L^{-1} had resulted in a decline of adsorption efficiency of GONP (Fig. 3a). According to Banerjee et al. [46], saturation of available active adsorption sites present on adsorbent surfaces has been considered responsible for an overall decrease in rate of adsorption with a parallel increase in adsorbate concentration.

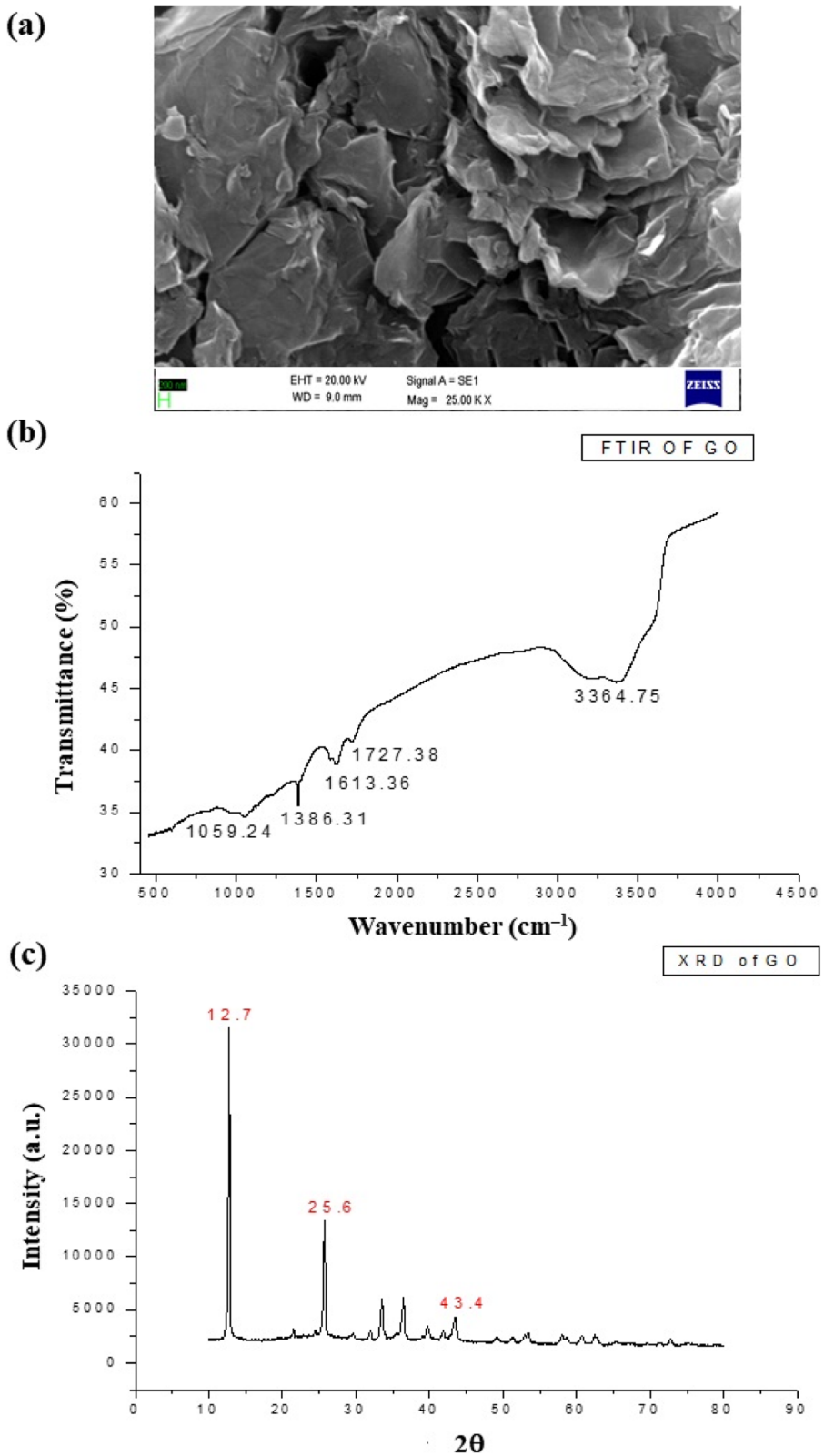

Fig. 2 Characterization of graphene oxide (GO). Plots (**a**–**c**) show the SEM image, the FTIR spectrum and the XRD spectrum of GO used in this study respectively

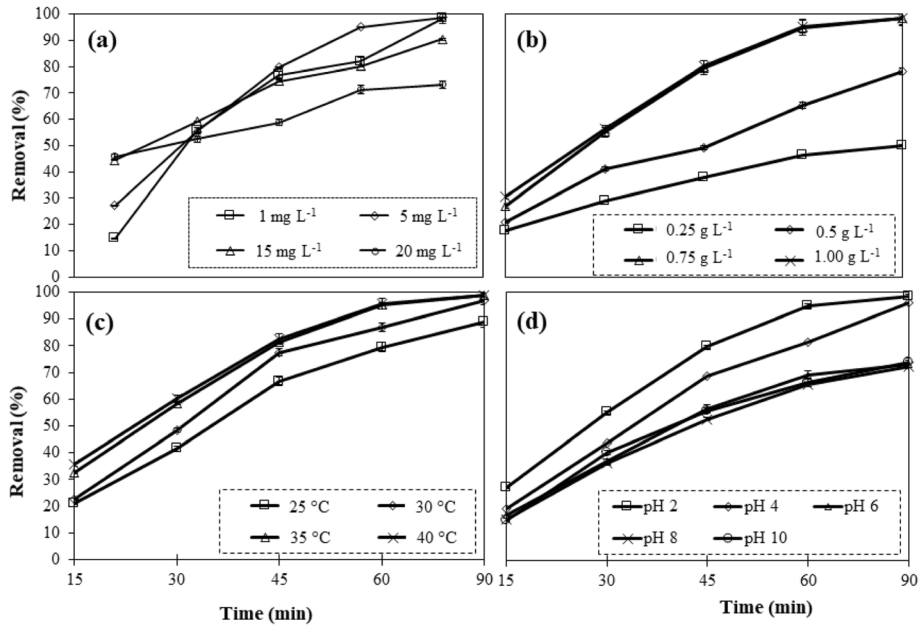

Fig. 3 Effect of experimental parameters on Carbamazepine (CBZ) adsorption over graphene oxide (GO). Plots (**a**–**d**) depict effect of variable initial CBZ concentration, GO dosage, experimental temperature and solution pH on rate of CBZ adsorption respectively

Effect of adsorbent dosage on adsorption efficiency

As shown in Fig. 3b, CBZ removal by GONP was found to increase from 50 to 99%, with a parallel increase in adsorbent dosage from 0.25–1.00 g L^{-1}, whereby the other experimental conditions were kept constant. An increase in the dosage of the adsorbent reportedly provides a higher number of active adsorption sites which in turn facilitates an increased adsorbate (CBZ) uptake [23, 47]. Results obtained in this study also established a direct proportionality between the dose of adsorbent and rate of adsorbate uptake.

Effect of temperature on adsorption efficiency

As shown in Fig. 3c, % removal of CBZ increased with a simultaneous increase in experimental temperature. Maximum removal (99%) of CBZ was recorded at 35 °C. Rise in temperature reportedly caused an increase of total pore volume and porosity of GONP particles [23]. This in turn facilitated higher rates of adsorption. However, a decline of % CBZ removal was observed with a further increase in temperature. According to previous studies, this had resulted due to the weakening of bonds between the adsorbate and the adsorbent moieties at temperatures exceeding 35 °C [23]. Increase in rate of adsorption with a corresponding rise in temperature is also considered indicative of endothermic nature of the adsorption process [23, 31].

Effect of solution pH on adsorption efficiency

CBZ adsorption by GONP is reportedly mediated via π-π interactions, electrostatic interactions and hydrophobic effects depending on the proximity of the bonding molecules [44]. The pKa value of CBZ is 13.9 [48, 49]. Therefore, under pH values lower than pKa values, CBZ present in protonated form reportedly facilitates uptake of the same by adsorbent particles [47]. pH of experimental solutions also influences functional groups present on the surface of both CBZ ($-NH_2$) and GONP (–OH, –COOH, –C-O, –C=O) [48]. Results obtained in batch studies (Fig. 3d) indicated that % removal of CBZ decreased with a corresponding increase in solution pH. A maximum CBZ uptake of 99% was obtained at pH 2. The pH_{pzc} of GO is 4.87 ± 0.26 [26]. At pH values lower than pH_{pzc}, GONP surface reportedly acquires positive charge [26] and is therefore capable of efficient removal of neutral CBZ moieties from aqueous solutions. According to similar studies, the decline in % removal of CBZ recorded at higher pH had resulted from hydrophobicity of CBZ exhibited at these pH conditions [48].

Process optimization using RSM

Results obtained for 20 experiments suggested by the RSM model developed on the basis of the aforementioned equation are shown in Table 1. The significance ($p < 0.0001$) of the model was indicated by a F-value as high as 851. Regression coefficient R^2 (0.999), the adjusted R^2 (0.998) and the predicted R^2 (0.998) obtained for CBZ adsorption by GONP established the best fit of this quadratic polynomial model over other tested models (like linear, cubic, two factor interaction) for predicting the results of the concerned study. An A_{deq}

precision value of 120 suggested that the selected model predicted % CBZ removal on the basis of a semi-empirical equation.

The % CBZ removal predicted by the model is shown in Table 1 along with those obtained experimentally. According to the results shown in Table 1, a good fit has been observed between both predicted and experimentally recorded values for each of the 20 experiments suggested by the developed model. The RSM (CCD) optimized conditions for CBZ adsorption were: adsorbent (GONP) dosage of 1 g L^{-1}, solution pH of 2 and treatment period of 120 min. Under these conditions, a maximum CBZ removal of 99% was achieved. The effect of interactions between the parameters selected for this study on the adsorption of CBZ by GONPs have been depicted in 3D plots shown in Fig. 4a-c and described as follows. The best fit curve between RSM model predicted and experimentally obtained data having an R^2 value of 0. 9992 has been shown in Supplementary Fig. S1a.

Effect of GONP dosage and solution pH on CBZ removal

The interaction of adsorbent dosage and solution pH on CBZ uptake by GONPs is shown in Fig. 4a. Under acidic conditions (pH 2–6) the rate of CBZ adsorption using GONP was found to increase with a parallel increase in adsorbent dosage (up to 1 g L^{-1}). Under acidic conditions, the surface of the GONPs acquired positive charge and hence was efficient in adsorbing neutral CBZ molecules [26, 46]. However, in keeping with recent studies, a decrease in CBZ uptake with parallel increase in adsorbent dosage beyond 1 g L^{-1} had occurred due to aggregation of adsorbent particles and resultant decrease in adsorptive surface area [22, 46].

Effect of interaction between solution pH and contact time on CBZ removal

The effect of pH and contact time on CBZ uptake by GONP is shown in Fig. 4b. Under acidic conditions, CBZ uptake by GONP was found to increase with a

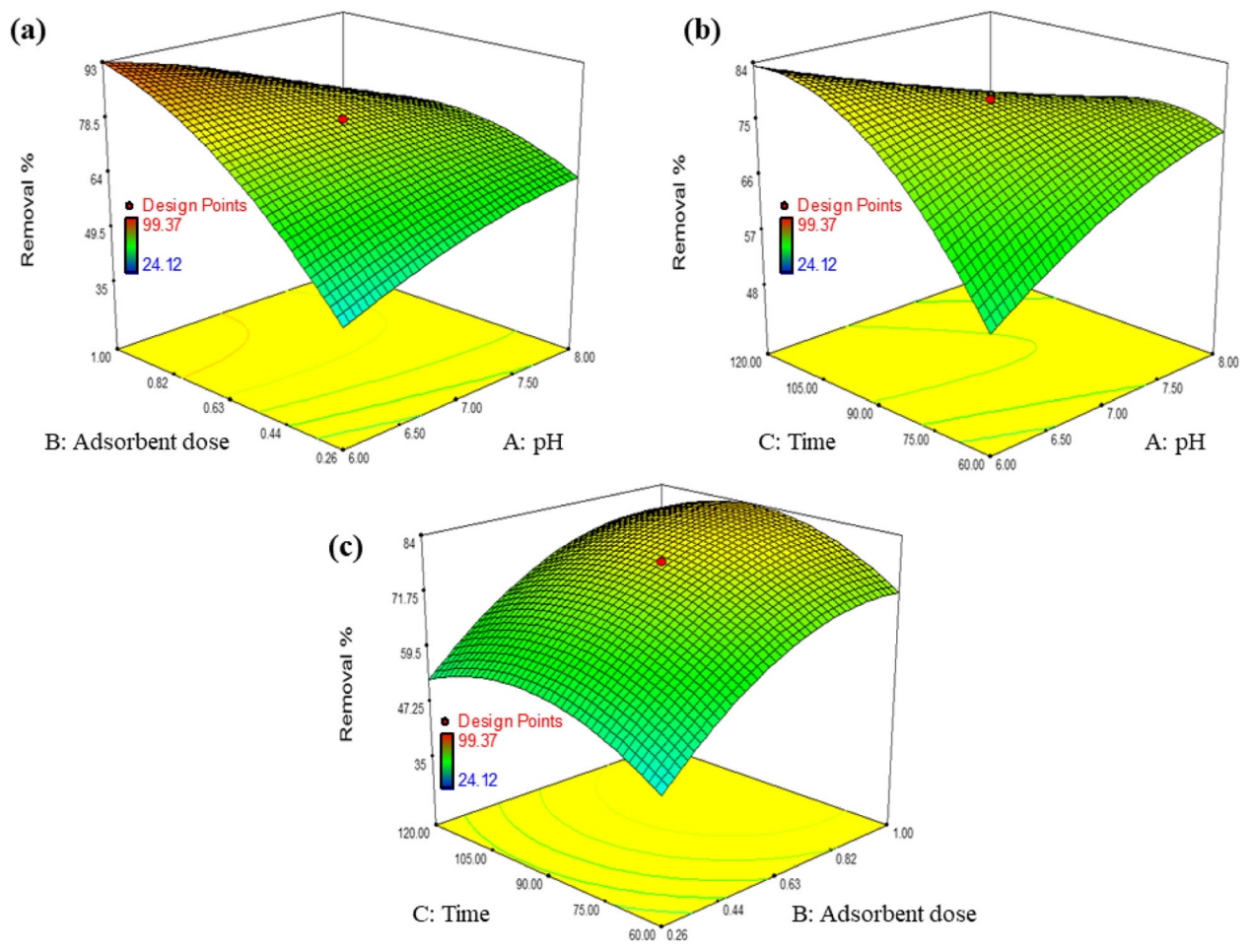

Fig. 4 Inter-parameter interactions and process optimization guiding Carbamazepine (CBZ) adsorption over graphene oxide (GO). Plots (**a**–**c**) show 3D plots illustrating impact of interactions of GO dosage vs. solution pH, solution pH vs. contact time and GO dosage vs. contact time on % CBZ removal respectively

simultaneous increase in contact time for 120 min. However, increase in solution pH was found to cause a decline in rate of CBZ uptake by GONP. With further increase in pH the adsorption of CBZ showed a decline due to accumulation of similar charges (neutral) on both adsorbent and adsorbate moieties [50]. No further increase in CBZ adsorption was observed beyond a contact time of 120 min.

Effect of interaction between GONP dosage and contact time on CBZ removal

The interaction of adsorbent dosage and contact time on CBZ uptake by GONP is shown in Fig. 4c. % CBZ removal was observed to increase with a parallel increase in both contact time and adsorbent dosage. This increase in % CBZ removal had occurred due to availability of larger number of active adsorption sites. However, the number of available adsorption sites had gradually decreased with time and acquired equilibrium conditions after a treatment period of 120 min [23].

Comparison of process optimization using RSM and ANN

The plot of the trained ANN model has been shown in Supplementary Fig. S1b. The R^2 for the trained ANN model and that suggested by RSM were found to be 0.998 and 0.999, respectively. Therefore, a higher correlation co-efficiency observed between the results predicted theoretically and obtained experimentally in case of RSM (CCD) modelling indicates that RSM is a better tool for optimization of the concerned process in comparison to ANN.

Process isotherms

% CBZ removal were fitted to different process isotherms like Langmuir, Freundlich, Temkin and Dubinin-Radushkevich models. As best results for each model was recorded with an adsorbent dosage of $1\ g\ L^{-1}$, only these results are shown in Table 2. Results obtained in batch studies showed best fit to Temkin isotherm as indicated by the values of R^2 shown in Table 2. Hence, it may be inferred that adsorption of CBZ by GONP was uniform in nature. Moreover, this also suggested that the heat of adsorption of the adsorbent moieties decreased in a linear fashion as the reaction proceeded [51].

Process kinetics

% CBZ removals recorded over a range of experimental temperatures (25–40 °C) were fitted to different models for analysis of process kinetics. The respective model constants and calculated R^2 are given in Table 3. As best results for each model was recorded with a temperature of 40 °C, only these results are shown in Table 3. Results obtained in batch studies showed best fit to the pseudo-second order kinetic model as shown in Table 3. The activation energy (E_a) calculated using the Arrhenius equation was found to be $78\ kJ\ mol^{-1}$ for the adsorption of CBZ by GONPS. An E_a value exceeding $40\ kJ\ mol^{-1}$ suggested that CBZ adsorption by GONP was chemisorption in nature [48]. Moreover, an increase in adsorption capacity ($2.4–2.7\ mg\ g^{-1}$) with a corresponding rise in temperature (25–40 °C) indicated the endothermic nature of the concerned process as well [46].

Process thermodynamics

According to results obtained, the values of Gibbs Free Energy (ΔG°) were found to decrease (− 4385 to − 16, $793\ kJ\ mol^{-1}$) with a parallel increase in temperature (25–40 °C). Negative values recorded for ΔG° indicated the spontaneous nature of the concerned process [48]. Moreover, the positive value obtained for enthalpy ($295\ kJ\ mol^{-1}$) confirmed the endothermic nature of the concerned process [46]. Besides, the positive value obtained for entropy ($856\ J\ mol^{-1}\ K^{-1}$) suggested that the translational entropy of the CBZ ions released was lower than that of the displaced water molecules and had resulted in a higher randomness at the interface of the adsorbate and the adsorbent [46].

Reusability study

Results indicated that best regeneration of adsorbent was obtained using NaOH (10 vol%) solution. The CBZ adsorption efficiency of GONP was found to remain the same for eight consecutive cycles and decline in the last two cycles (95 and 90% removal efficiency, respectively). This had occurred due to mass loss from handling or degeneration of adsorbent surface resulting from repeated regeneration using NaOH (10 vol% solution) [24].

Conclusions

This study investigated the potential of GONP for adsorptive removal of CBZ from aqueous solutions. The GONPs reported in this study demonstrated a maximum CBZ adsorption capacity of $9.2\ mg\ g^{-1}$. The process of adsorption reported herein was found to be guided by Temkin isotherm and pseudo-second order kinetics. The process was also found to be endothermic and spontaneous in nature. RSM (CCD) was found to be a more efficient tool for optimization of the concerned process in comparison to ANN. A maximum adsorbate removal of 99% was recorded from a solution containing $5\ mg\ L^{-1}$ of CBZ under optimized conditions of solution pH (2), adsorbent dosage ($1\ g\ L^{-1}$) and contact time (120 min). The RSM optimization conducted in this study also provided novel information regarding the interactions occurring between adsorbent and adsorbate moieties during the process of adsorption. Moreover, this study also established that GO is an efficient adsorbent by

virtue of its requirement in extremely small dosages and high reusability potential in comparison to other contemporary adsorbents reported in literature. GONP reported in this study may be investigated further for efficient treatment of real effluents bearing multiple pollutants.

Supplementary information

Supplementary information accompanies this paper at https://doi.org/10.1186/s42834-020-00062-8.

Additional file 1: Fig. S1. Predicted % CBZ removal vs. experimentally recorded % CBZ. Plots (a) and (b) show results obtained from RSM (CCD) and ANN analysis respectively.

Acknowledgements
All authors are thankful to Department of Chemical Engineering Jadavpur University and Department of Chemical Engineering, Indian Institute of Technology – Guwahati. Authors are also thankful to Department of Science & Technology, Water Technology Initiative for funding the project.

Authors' contributions
SB and PB had planned and performed the experiments and written the manuscript. PD and AB supervised the project in consultation with SKM and PG. All authors read and approved the manuscript.

Funding
All authors are thankful to Department of Science and Technology – Water Technology Initiative, Government of India, for the financial support (Ref: DST/TM/WTI/2 K16/20 (G), Research Grant-in Aid).

Availability of data and materials
All experimental data generated and used in the manuscript are with authors and will be provided on request to authors.

Competing interests
The authors declare that they have no financial and non-financial competing interests.

Author details
[1]Department of Chemical Engineering, Jadavpur University, Kolkata 700032, India. [2]Department of Environmental Studies, Rabindra Bharati University, Kolkata 700091, India. [3]School of Advanced Studies in Industrial Pollution Control Engineering, Jadavpur University, Kolkata 700032, India. [4]Department of Chemical Engineering, Indian Institute of Technology, Guwahati 781039, India.

Received: 30 March 2020 Accepted: 20 August 2020
Published online: 04 September 2020

References
1. Daghrir R, Drogui P, Dimboukou-Mpira A, El Khakani MA. Photoelectrocatalytic degradation of carbamazepine using Ti/TiO_2 nanostructured electrodes deposited by means of a pulsed laser deposition process. Chemosphere. 2013;93:2756–66.
2. Martin-Diaz L, Franzellitti S, Buratti S, Valbonesi P, Capuzzo A, Fabbri E. Effects of environmental concentrations of the antiepilectic drug carbamazepine on biomarkers and cAMP-mediated cell signaling in the mussel *Mytilus galloprovincialis*. Aquat Toxicol. 2009;94:177–85 .
3. Mohapatra DP, Brar SK, Daghrir R, Tyagi RD, Picard P, Surampalli RY, et al. Photocatalytic degradation of carbamazepine in wastewater by using a new class of whey-stabilized nanocrystalline TiO_2 and ZnO. Sci Total Environ. 2014;485–6:263–9.
4. Scheytt T, Mersmann P, Lindstadt R, Heberer T. 1-octanol/water partition coefficients of 5 pharmaceuticals from human medical care: carbamazepine, clofibric acid, diclofenac, ibuprofen, and propyphenazone. Water Air Soil Poll. 2005;165:3–11.
5. Chong MN, Jin B. Photocatalytic treatment of high concentration carbamazepine in synthetic hospital wastewater. J Hazard Mater. 2012; 199–200:135–42.
6. Miao XS, Metcalfe CD. Determination of carbamazepine and its metabolites in aqueous samples using liquid chromatography-electrospray tandem mass spectrometry. Anal Chem. 2003;75:3731–8.
7. Zhang YJ, Geissen SU, Gal C. Carbamazepine and diclofenac: removal in wastewater treatment plants and occurrence in water bodies. Chemosphere. 2008;73:1151–61.
8. Calisto V, Domingues MRM, Erny GL, Esteves VI. Direct photodegradation of carbamazepine followed by micellar electrokinetic chromatography and mass spectrometry. Water Res. 2011;45:1095–104.
9. Metcalfe CD, Koenig BG, Bennie DT, Servos M, Ternes TA, Hirsch R. Occurrence of neutral and acidic drugs in the effluents of Canadian sewage treatment plants. Environ Toxicol Chem. 2003;22:2872–80.
10. Focazio MJ, Kolpin DW, Barnes KK, Furlong ET, Meyer MT, Zaugg SD, et al. A national reconnaissance for pharmaceuticals and other organic wastewater contaminants in the United States - II untreated drinking water sources. Sci Total Environ. 2008;402:201–16.
11. Lapworth DJ, Baran N, Stuart ME, Ward RS. Emerging organic contaminants in groundwater: a review of sources, fate and occurrence. Environ Pollut. 2012;163:287–303.
12. Hummel D, Loffler D, Fink G, Ternes TA. Simultaneous determination of psychoactive drugs and their metabolites in aqueous matrices by liquid chromatography mass spectrometry. Environ Sci Technol. 2006;40:7321–8.
13. Bahlmann A, Weller MG, Panne U, Schneider RJ. Monitoring carbamazepine in surface and wastewaters by an immunoassay based on a monoclonal antibody. Anal Bioanal Chem. 2009;395:1809–20.
14. Heberer T, Reddersen K, Mechlinski A. From municipal sewage to drinking water: fate and removal of pharmaceutical residues in the aquatic environment in urban areas. Water Sci Technol. 2002;46:81–8.
15. Ferrari B, Paxeus N, Lo Giudice R, Pollio A, Garric J. Ecotoxicological impact of pharmaceuticals found in treated wastewaters: study of carbamazepine, clofibric acid, and diclofenac. Ecotox Environ Safe. 2003;55:359–70.
16. Hai FI, Yang SF, Asif MB, Sencadas V, Shawkat S, Sanderson-Smith M, et al. Carbamazepine as a possible anthropogenic marker in water: occurrences, toxicological effects, regulations and removal by wastewater treatment technologies. Water-Sui. 2018;10:107.
17. Kinney CA, Furlong ET, Zaugg SD, Burkhardt MR, Werner SL, Cahill JD, et al. Survey of organic wastewater contaminants in biosolids destined for land application. Environ Sci Technol. 2006;40:7207–15.
18. Chen F, Ying GG, Kong LX, Wang L, Zhao JL, Zhou LJ, et al. Distribution and accumulation of endocrine-disrupting chemicals and pharmaceuticals in wastewater irrigated soils in Hebei, China. Environ Pollut. 2011;159:1490–8.
19. Fernandez-Lopez C, Guillen-Navarro JM, Padilla JJ, Parsons JR. Comparison of the removal efficiencies of selected pharmaceuticals in wastewater treatment plants in the region of Murcia, Spain Ecol Eng. 2016;95:811–6.
20. Banerjee P, Dey TK, Sarkar S, Swarnakar S, Mukhopadhyay A, Ghosh S. Treatment of cosmetic effluent in different configurations of ceramic UF membrane based bioreactor: toxicity evaluation of the untreated and treated wastewater using catfish (*Heteropneustes fossilis*). Chemosphere. 2016;146:133–44.
21. Liu L, Li C, Bao CL, Jia Q, Xiao PF, Liu XT, et al. Preparation and characterization of chitosan/graphene oxide composites for the adsorption of Au (III) and Pd(II). Talanta. 2012;93:350–7.
22. Banerjee P, Sau S, Das P, Mukhopadhayay A. Optimization and modelling of synthetic azo dye wastewater treatment using Graphene oxide nanoplatelets: characterization toxicity evaluation and optimization using artificial neural network. Ecotox Environ Safe. 2015;119:47–57.
23. Banerjee P, Das P, Zaman A, Das P. Application of graphene oxide nanoplatelets for adsorption of ibuprofen from aqueous solutions: evaluation of process kinetics and thermodynamics. Process Saf Environ. 2016;101:45–53.
24. Li YH, Du QJ, Liu TH, Peng XJ, Wang JJ, Sun JK, et al. Comparative study of methylene blue dye adsorption onto activated carbon, graphene oxide, and carbon nanotubes. Chem Eng Res Des. 2013;91:361–8.
25. Travlou NA, Kyzas GZ, Lazaridis NK, Deliyanni EA. Graphite oxide/chitosan composite for reactive dye removal. Chem Eng J. 2013;217:256–65.
26. Banerjee P, Mukhopadhyay A, Das P. Graphene oxide-nanobentonite composite sieves for enhanced desalination and dye removal. Desalination. 2019;451:231–40.

27. Das P, Banerjee P, Rathour R, Misra R. Assessment on linear and non-linear analysis for the estimation of pseudo-second-order kinetic parameters for removal of dye using graphene nanosheet. Desalin Water Treat. 2015;56:502–8.
28. Senthilkumar S, Prabhu HJ, Perumalsamy M. Response surface optimization for biodegradation of textile azo dyes using isolated bacterial strain *Pseudomonas* sp. Arab J Sci Eng. 2013;38:2279–91.
29. Banerjee P, Mukhopadhayay A, Das P. Advances in bioremediation for removal of toxic dye from different streams of wastewater. In: Rathoure AK, Dhatwalia VK, editors. Toxicity and waste management using bioremediation. Hershey: IGI Global; 2016. p. 266–78.
30. Aghav RM, Kumar S, Mukherjee SN. Artificial neural network modeling in competitive adsorption of phenol and resorcinol from water environment using some carbonaceous adsorbents. J Hazard Mater. 2011;188:67–77.
31. Bhattacharyya S, Banerjee P, Bhattacharya S, Rathour RKS, Majumder SK, Das P, et al. Comparative assessment on the removal of ranitidine and prednisolone present in solution using graphene oxide (GO) nanoplatelets. Desalin Water Treat. 2018;132:287–96.
32. Hanaor DAH, Ghadiri M, Chrzanowski W, Gan YX. Scalable surface area characterization by electrokinetic analysis of complex anion adsorption. Langmuir. 2014;30:15143–52.
33. Ghaedi M, Ansari A, Habibi MH, Asghari AR. Removal of malachite green from aqueous solution by zinc oxide nanoparticle loaded on activated carbon: kinetics and isotherm study. J Ind Eng Chem. 2014;20:17–28.
34. Ghaedi M, Ansari A, Bahari F, Ghaedi AM, Vafaei A. A hybrid artificial neural network and particle swarm optimization for prediction of removal of hazardous dye brilliant green from aqueous solution using zinc sulfide nanoparticle loaded on activated carbon. Spectrochim Acta A. 2015;137:1004–15.
35. Lagergren S. About the theory of so-called adsorption of soluble substances. Kungl Svenska Vetenskapsakad Handl. 1898;24:1–39 [in German].
36. Ho YS, McKay G. Pseudo-second order model for sorption processes. Process Biochem. 1999;34:451–65.
37. Mckay G. The adsorption of dyestuffs from aqueous solution using activated carbon: analytical solution for batch adsorption based on external mass transfer and pore diffusion. Chem Eng J. 1983;27:187–96.
38. Ho YS, McKay G. The kinetics of sorption of divalent metal ions onto sphagnum moss peat. Water Res. 2000;34:735–42.
39. Anirudhan TS, Radhakrishnan PG. Thermodynamics and kinetics of adsorption of Cu(II) from aqueous solutions onto a new cation exchanger derived from tamarind fruit shell. J Chem Thermodyn. 2008;40:702–9.
40. Saeed A, Sharif M, Iqbal M. Application potential of grapefruit peel as dye sorbent: kinetics, equilibrium and mechanism of crystal violet adsorption. J Hazard Mater. 2010;179:564–72.
41. Goswami S, Banerjee P, Datta S, Mukhopadhayay A, Das P. Graphene oxide nanoplatelets synthesized with carbonized agro-waste biomass as green precursor and its application for the treatment of dye rich wastewater. Process Saf Environ. 2017;106:163–72.
42. Mukherjee M, Goswami S, Banerjee P, Sengupta S, Das P, Banerjee PK, et al. Ultrasonic assisted graphene oxide nanosheet for the removal of phenol containing solution. Environ Technol Inno. 2019;13:398–407.
43. Wu NQ, Fu L, Su M, Aslam M, Wong KC, Dravid VP. Interaction of fatty acid monolayers with cobalt nanoparticles. Nano Lett. 2004;4:383–6.
44. Lim MS, Feng K, Chen XQ, Wu NQ, Raman A, Nightingale J, et al. Adsorption and desorption of stearic acid self-assembled monolayers on aluminum oxide. Langmuir. 2007;23:2444–52.
45. Pongpiachan S. FTIR spectra of organic functional group compositions in $PM_{2.5}$ collected at Chiang-Mai city, Thailand during the haze episode in March 2012. J Appl Sci. 2014;14:2967–77.
46. Banerjee P, Barman SR, Mukhopadhayay A, Das P. Ultrasound assisted mixed azo dye adsorption by chitosan-graphene oxide nanocomposite. Chem Eng Res Des. 2017;117:43–56.
47. Roy S, Das P, Sengupta S, Manna S. Calcium impregnated activated charcoal: optimization and efficiency for the treatment of fluoride containing solution in batch and fixed bed reactor. Process Saf Environ. 2017;109:18–29.
48. Al-Hamadani YAJ, Lee G, Kim S, Park CM, Jang M, Her N, et al. Sonocatalytic degradation of carbamazepine and diclofenac in the presence of graphene oxides in aqueous solution. Chemosphere. 2018;205:719–27.
49. Rohricht M, Krisam J, Weise U, Kraus UR, During RA. Elimination of carbamazepine, diclofenac and naproxen from treated wastewater by nanofiltration. Clean-Soil Air Water. 2009;37:638–41.
50. Cai N, Larese-Casanova P. Application of positively-charged ethylenediamine-functionalized graphene for the sorption of anionic organic contaminants from water. J Environ Chem Eng. 2016;4:2941–51.
51. Dada AO, Olalekan AP, Olatunya AM, Dada O. Langmuir, Freundlich, Temkin and Dubinin–Radushkevich isotherms studies of equilibrium sorption of Zn^{2+} unto phosphoric acid modified rice husk. IOSR J Appl Chem. 2012;3:38–45.

Publisher's Note